

# Supplementary materials

## **Mitigating the impact of image processing variations on tumour [ $^{18}\text{F}$ ]-FDG-PET radiomic feature robustness**

Syafiq Ramlee \*, Roido Manavaki, Luigi Aloj, Lorena Escudero Sanchez

\* Correspondence: Syafiq Ramlee, [masr4@cam.ac.uk](mailto:masr4@cam.ac.uk)

## Supplementary Table ST1

The number of features (and corresponding percentage proportion, out of the 107 features extracted) for each robustness category, stratified by intensity discretisation or voxel interpolation scheme and cancer type.

	Robust			Conditionally robust			Not robust		
	NSCLC	Melanoma	Lymphoma	NSCLC	Melanoma	Lymphoma	NSCLC	Melanoma	Lymphoma
<b>Discretisation</b>									
FBW	33 (30%)	31 (29%)	34 (32%)	41 (38%)	65 (61%)	59 (55%)	33 (31%)	11 (10%)	14 (13%)
FBN	36 (34%)	33 (31%)	34 (32%)	24 (22%)	35 (33%)	22 (21%)	47 (44%)	39 (36%)	51 (48%)
<b>Interpolation</b>									
Linear	38 (36%)	30 (28%)	35 (33%)	60 (56%)	67 (63%)	64 (60%)	9 (8%)	10 (9%)	8 (7%)
Nearest-neighbour	41 (38%)	31 (29%)	42 (39%)	61 (57%)	71 (66%)	60 (56%)	5 (5%)	5 (5%)	5 (5%)
B-spline	39 (36%)	31 (29%)	35 (33%)	57 (53%)	66 (62%)	64 (60%)	11 (10%)	10 (9%)	8 (7%)
Gaussian	39 (36%)	36 (34%)	38 (36%)	55 (51%)	61 (57%)	59 (55%)	13 (12%)	10 (9%)	10 (9%)



## Supplementary Table ST2

The number of features (and corresponding percentage proportion, out of the 107 features extracted) for each correctability category, stratified by intensity discretisation or voxel interpolation scheme and cancer type.

	Correctable			Moderately correctable			Not correctable		
	NSCLC	Melanoma	Lymphoma	NSCLC	Melanoma	Lymphoma	NSCLC	Melanoma	Lymphoma
<b>Discretisation</b>									
FBW	30 (28%)	22 (20%)	27 (25%)	37 (35%)	37 (35%)	40 (37%)	7 (7%)	17 (16%)	6 (6%)
FBN	30 (28%)	29 (27%)	32 (30%)	38 (36%)	34 (32%)	31 (29%)	3 (3%)	11 (10%)	10 (9%)
<b>Interpolation</b>									
Linear	30 (28%)	25 (23%)	29 (27%)	29 (27%)	36 (34%)	33 (30%)	10 (9%)	16 (15%)	10 (9%)
Nearest-neighbour	24 (22%)	16 (15%)	16 (15%)	27 (25%)	39 (36%)	36 (34%)	15 (14%)	21 (20%)	13 (12%)
B-spline	29 (27%)	23 (22%)	28 (26%)	30 (28%)	34 (32%)	30 (28%)	9 (8%)	19 (18%)	14 (13%)
Gaussian	31 (29%)	25 (23%)	28 (26%)	27 (25%)	27 (25%)	28 (26%)	10 (9%)	19 (18%)	13 (12%)

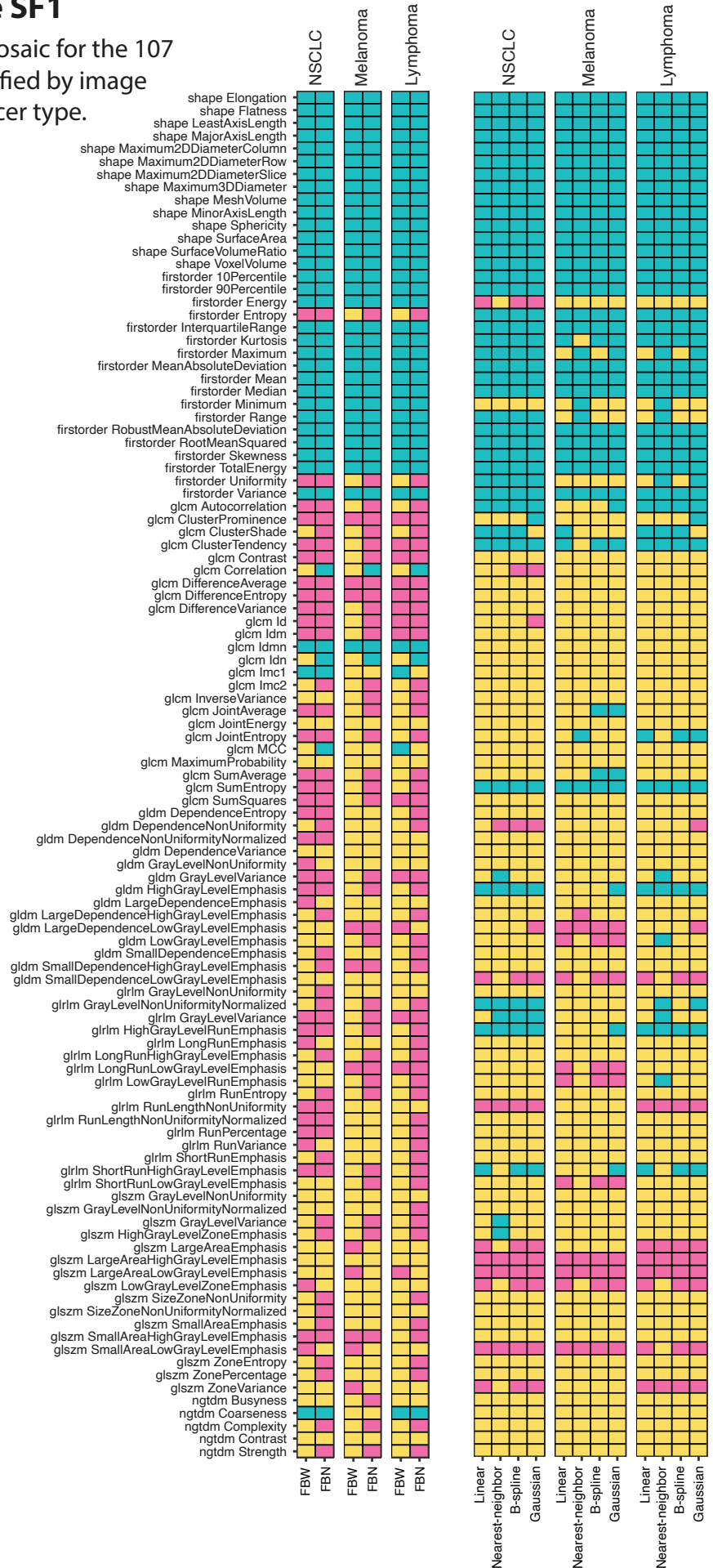
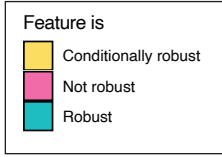
## Supplementary Table ST3

The most correctable feature for each intensity discretisation or voxel interpolation scheme, across the cancers investigated.

	<b>NSCLC</b>	<b>Melanoma</b>	<b>Lymphoma</b>
<b>Discretisation</b>			
FBW	GLCM DifferenceVariance	GLCM Contrast	GLCM Contrast
FBN	First-order Uniformity	GLCM ClusterTendency	First-order Uniformity
<b>Interpolation</b>			
Linear	First-order Energy	GLSZM ZonePercentage	First-order Energy
Nearest- neighbour	First-order Energy	First-order Energy	First-order Energy
B-spline	First-order Energy	GLSZM ZonePercentage	First-order Energy
Gaussian	First-order Energy	GLSZM ZonePercentage	First-order Energy

# Supplementary Figure SF1

Robustness categorisations mosaic for the 107 radiomic features tested, stratified by image processing algorithm and cancer type.







































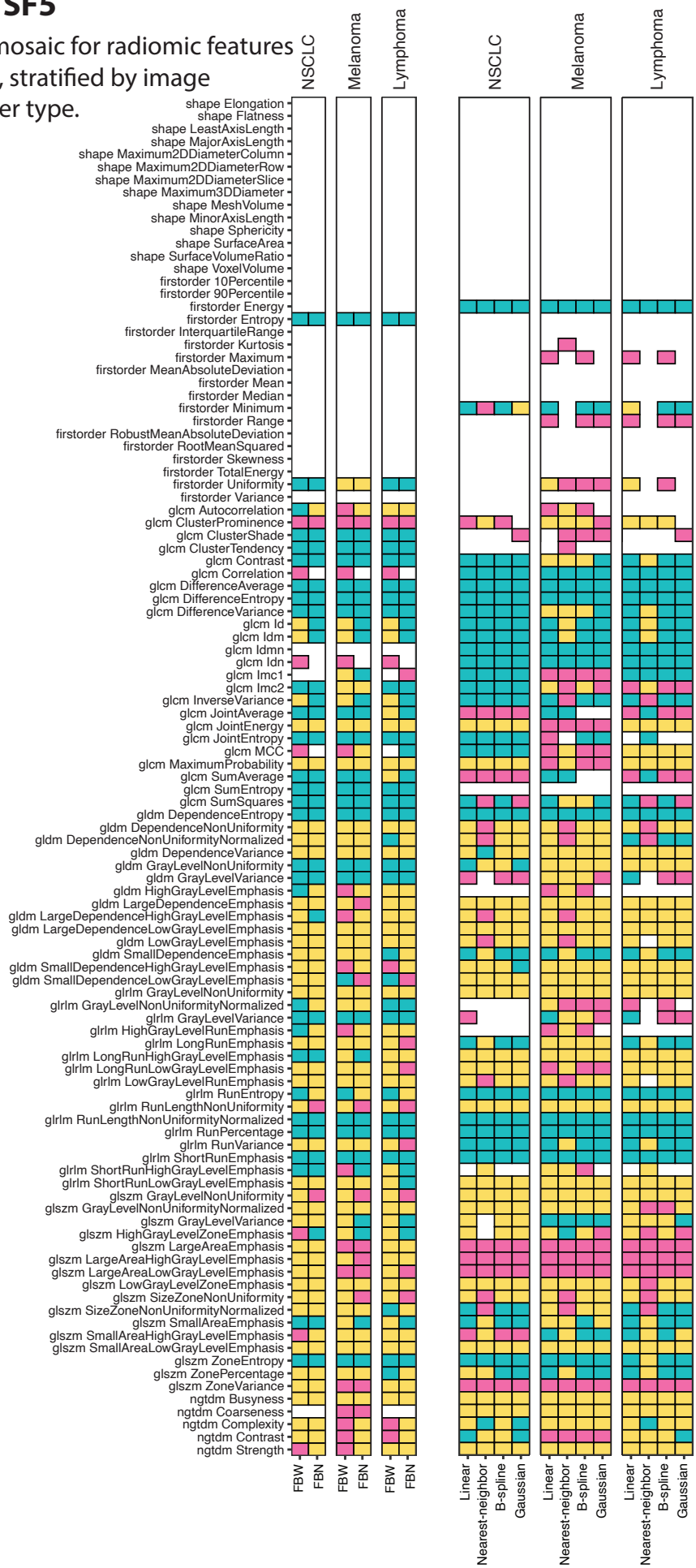
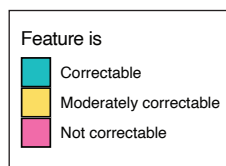






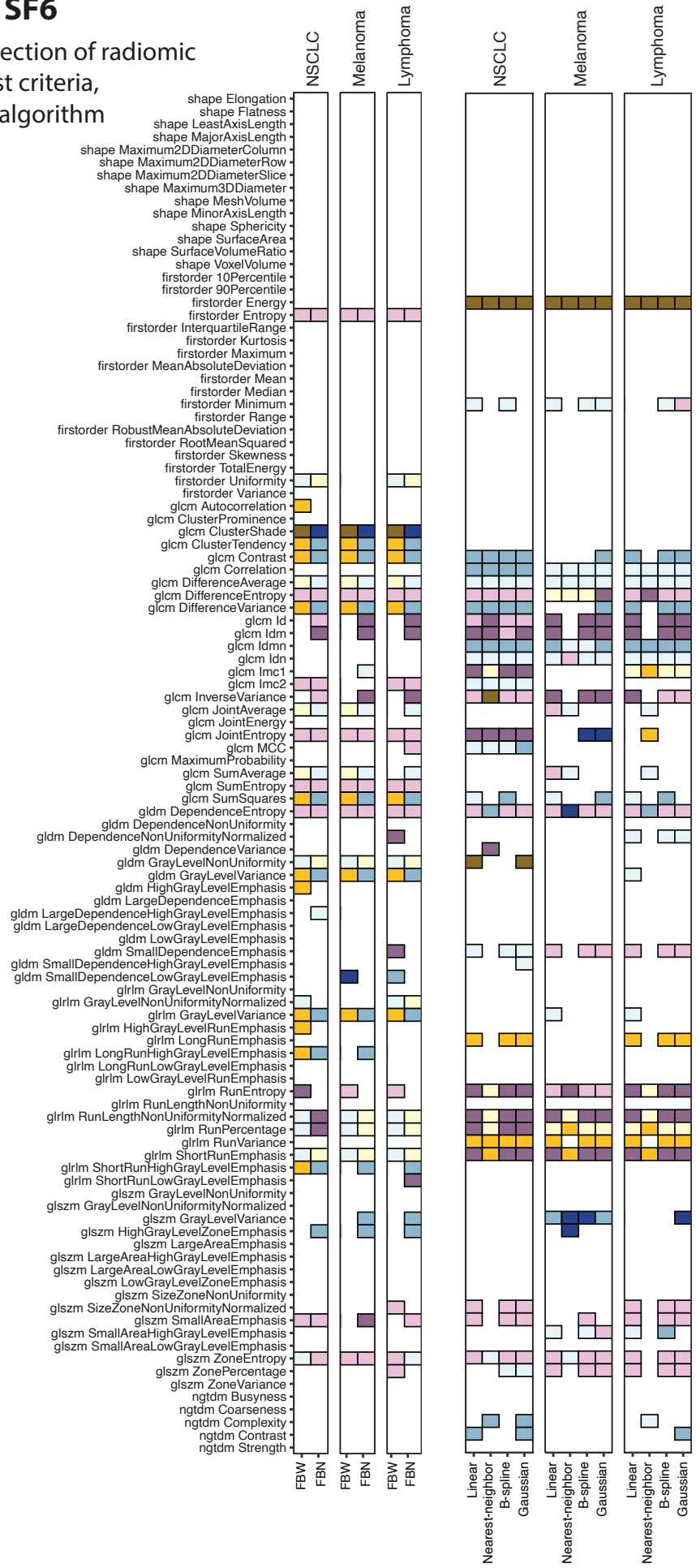
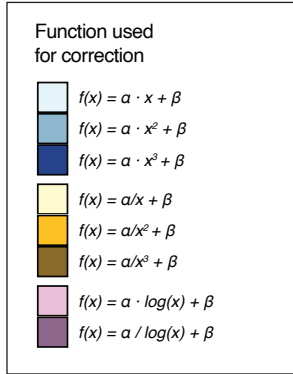
# Supplementary Figure SF5

Correctability categorisations mosaic for radiomic features not meeting the robust criteria, stratified by image processing algorithm and cancer type.



# Supplementary Figure SF6

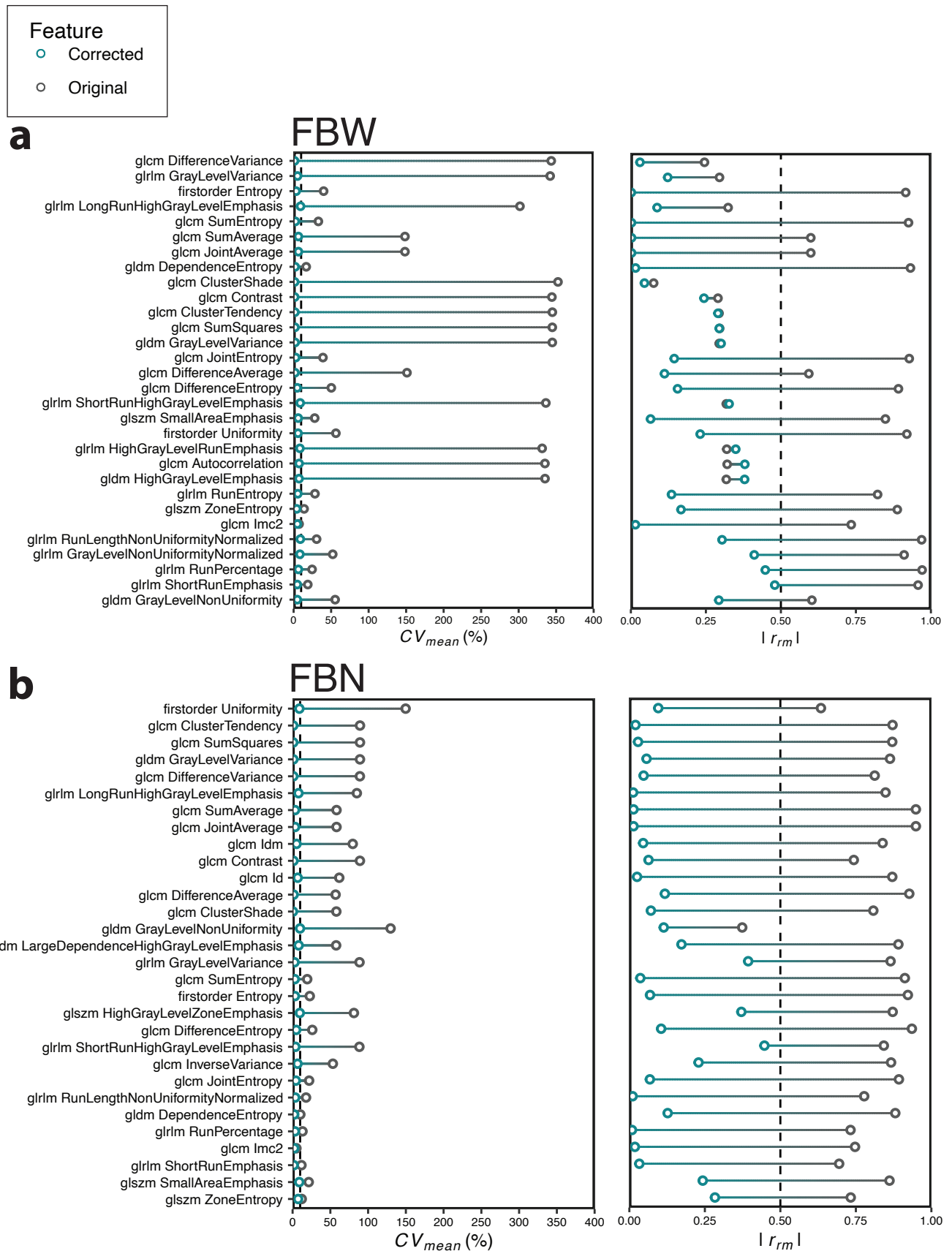
Best-fit equations used for correction of radiomic features not meeting the robust criteria, stratified by image processing algorithm and cancer type.



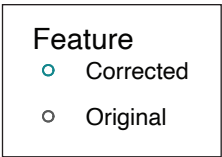


## Supplementary Figure SF7

Dumbbell plots showing the change in  $CV_{mean}$  and  $|r_{rm}|$  for correctable features in NSCLC, when considering the different discretisation (a-b) and interpolation (c-f) algorithms tested. Features are ranked by the change in feature variability and correlation upon correction.

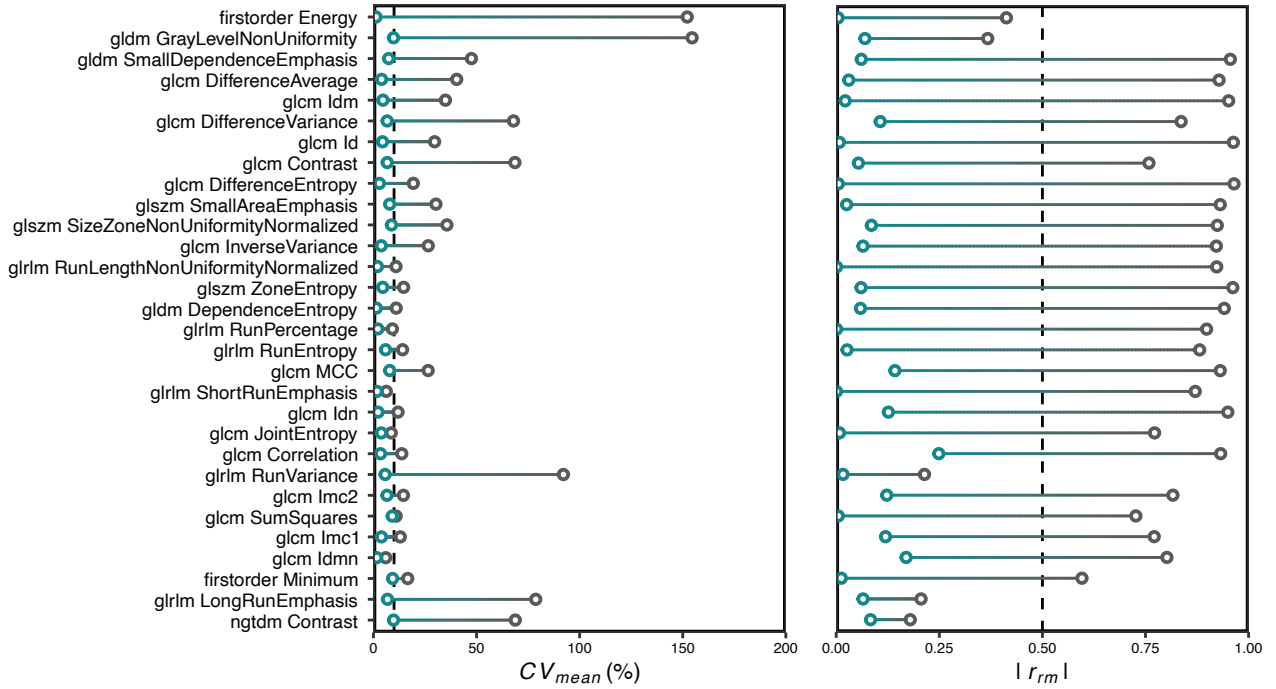






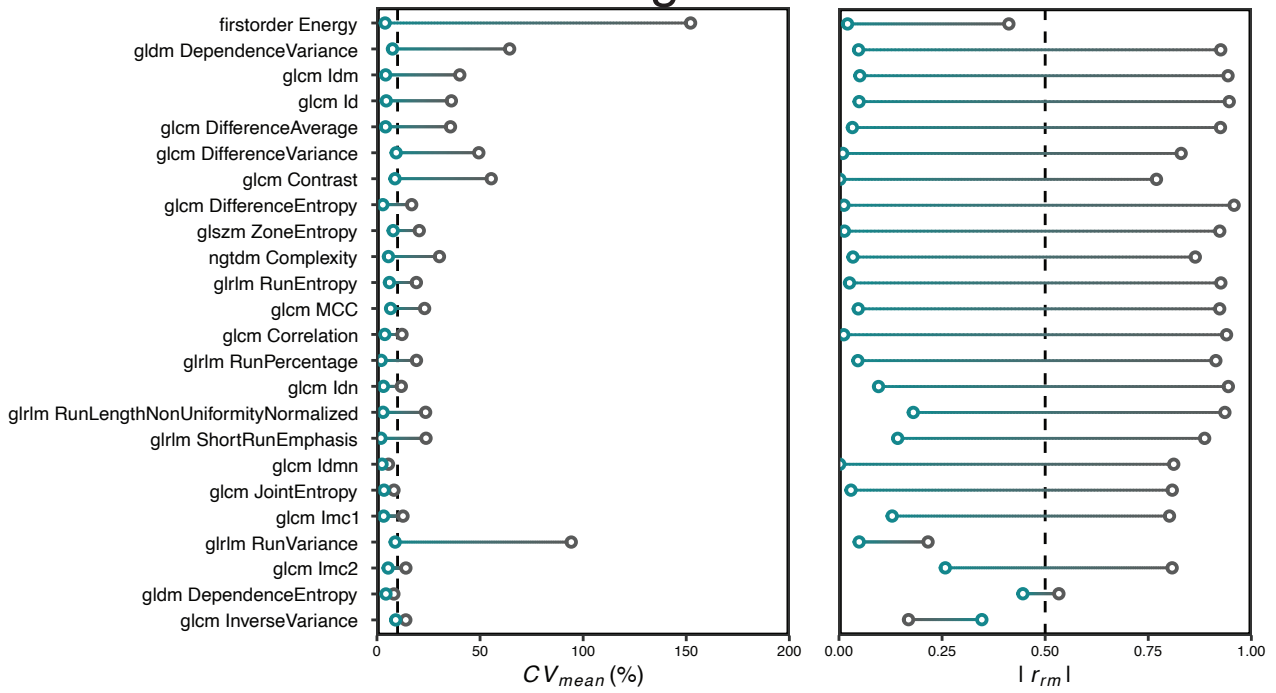
**c**

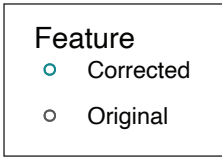
**Linear**



**d**

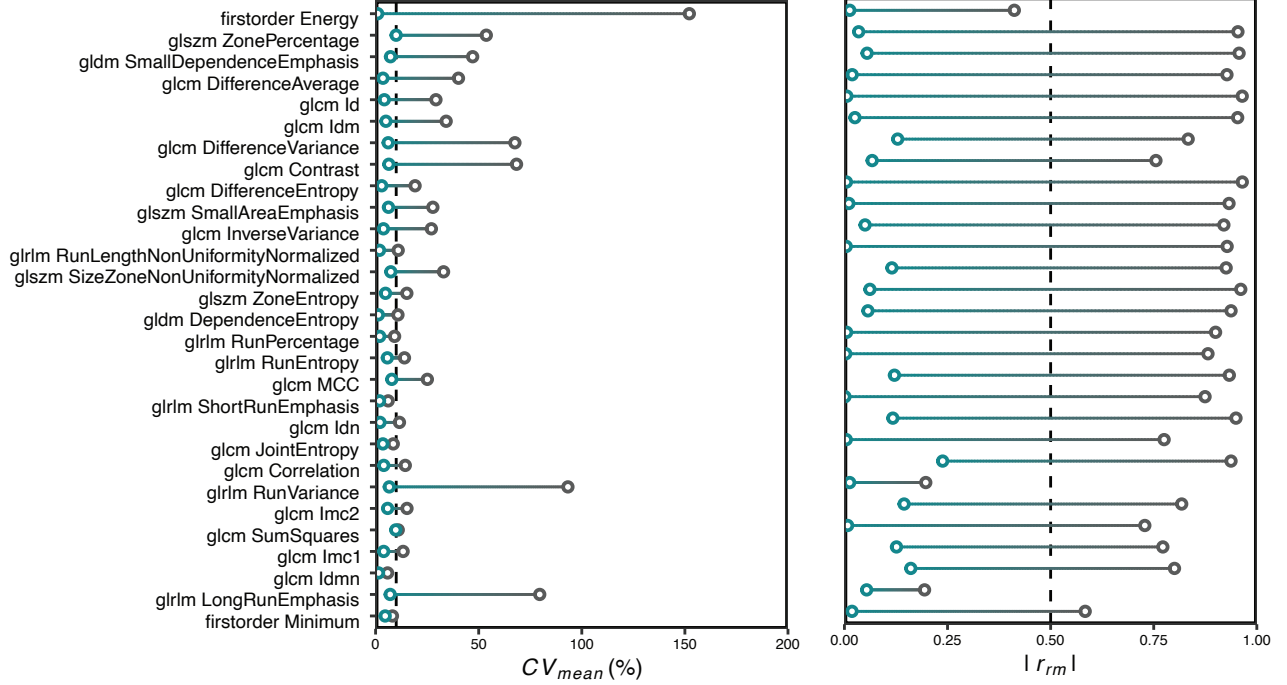
**Nearest-neighbour**





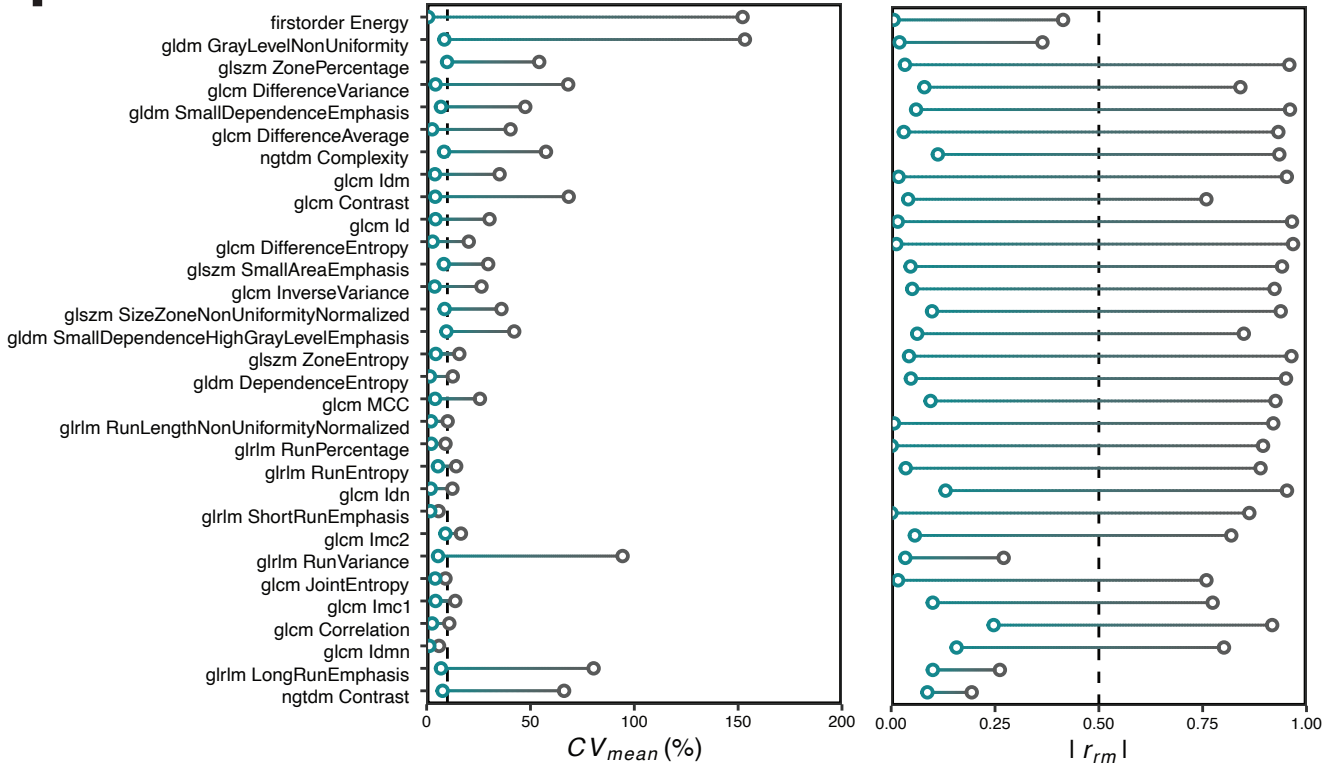
**e**

**B-spline**



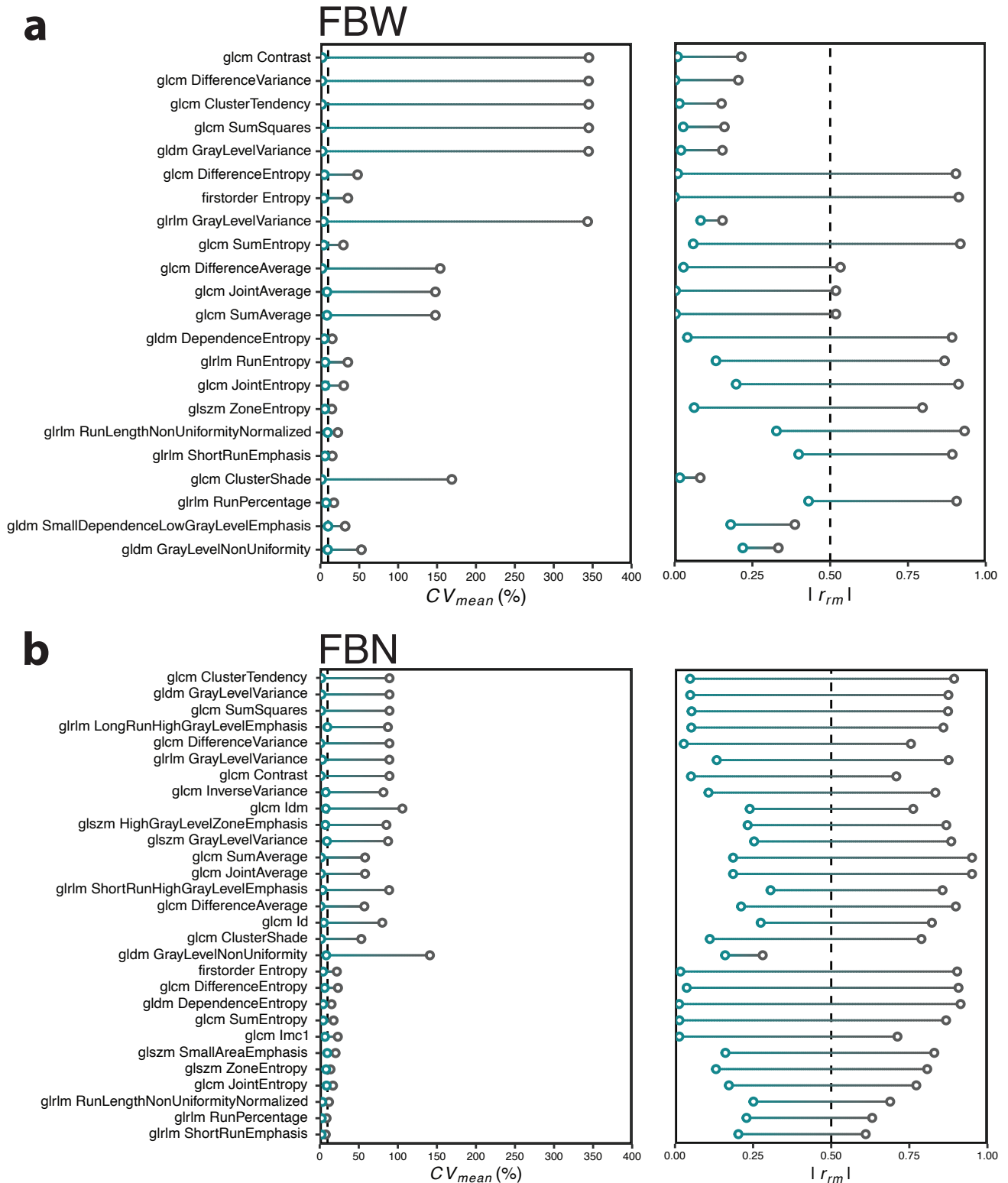
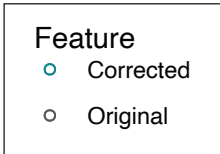
**f**

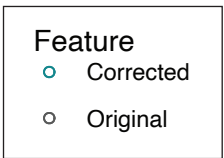
**Gaussian**



## Supplementary Figure SF8

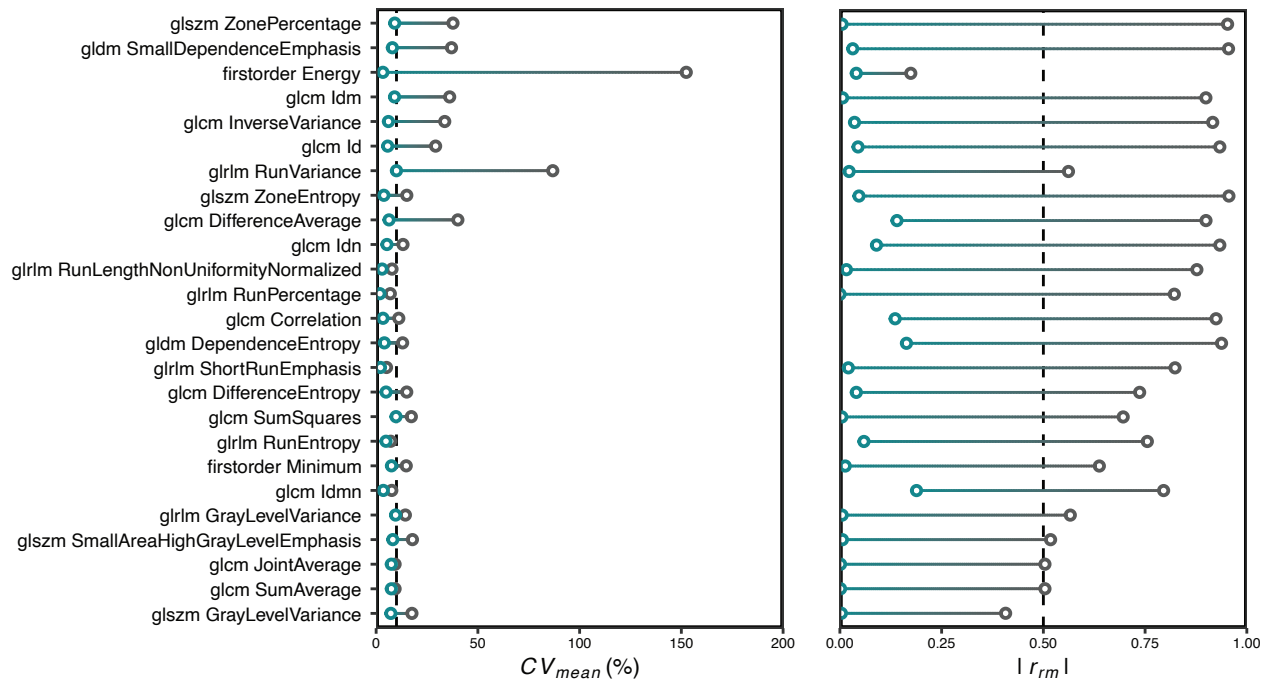
Dumbbell plots showing the change in  $CV_{mean}$  and  $|r_{rm}|$  for correctable features in melanoma, when considering the different discretisation (a-b) and interpolation (c-f) algorithms tested. Features are ranked by the change in feature variability and correlation upon correction.





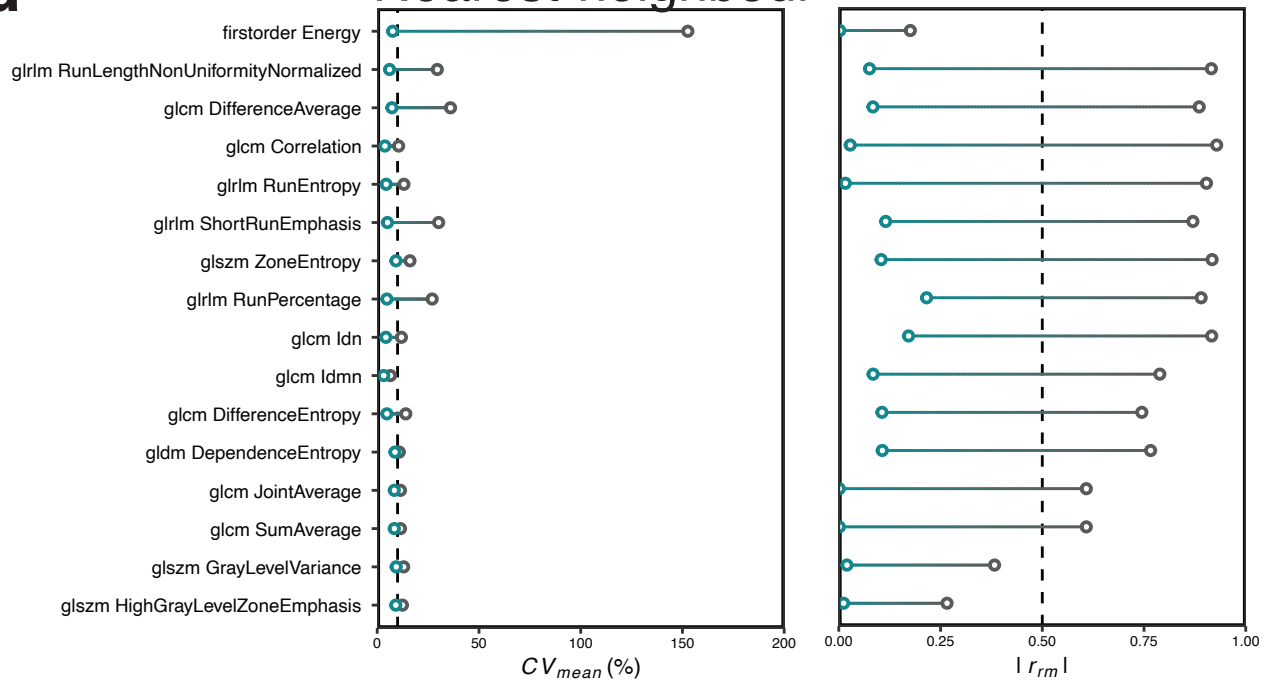
**c**

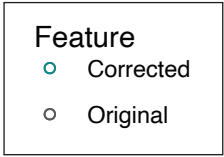
**Linear**



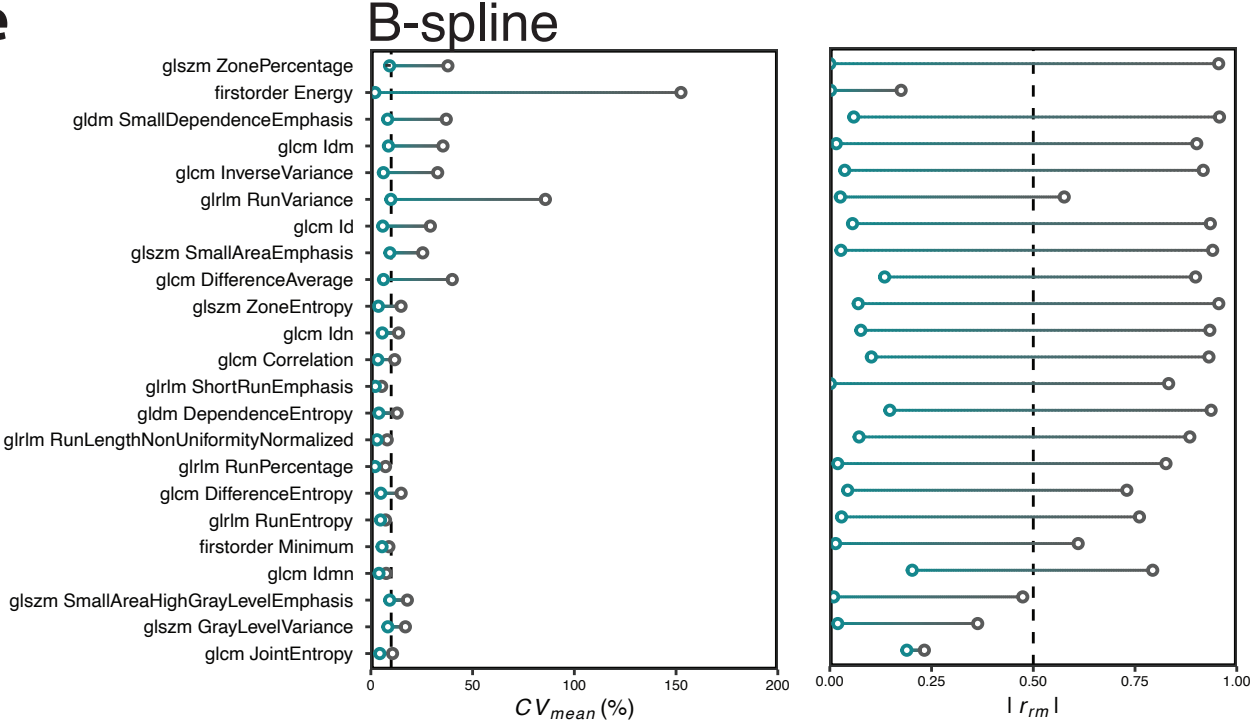
**d**

**Nearest-neighbour**

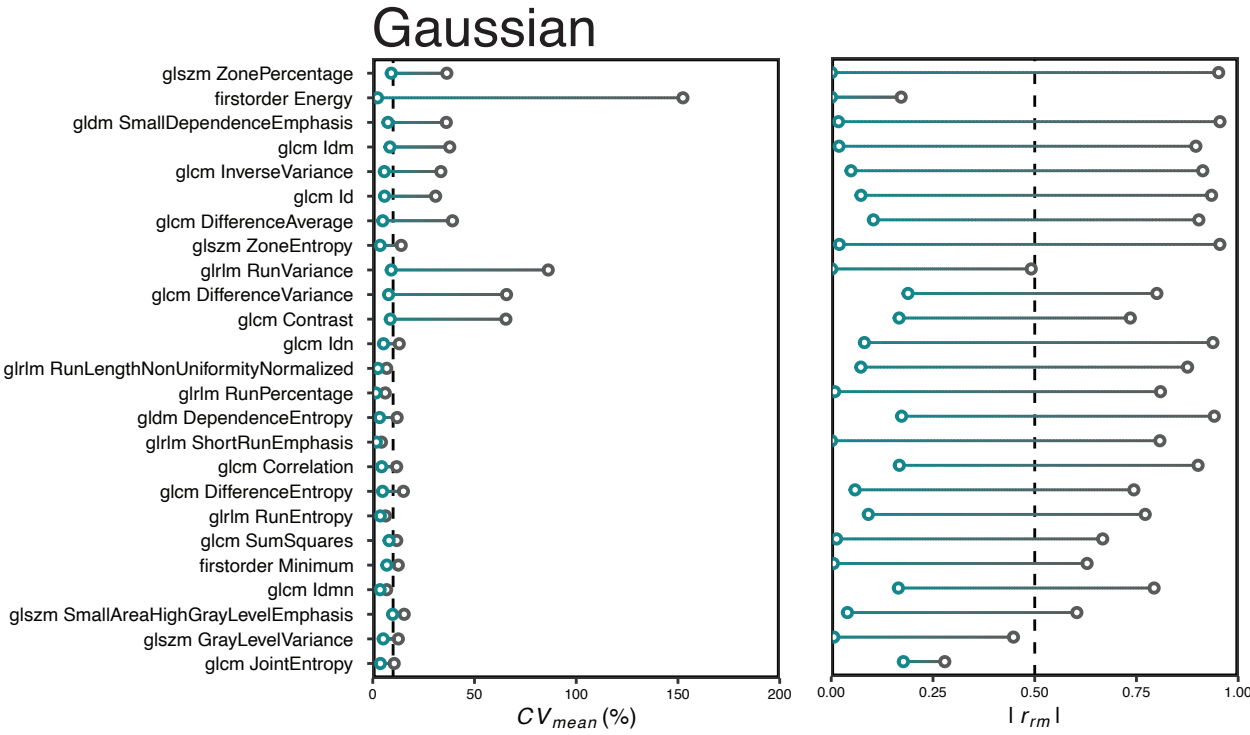




**e**

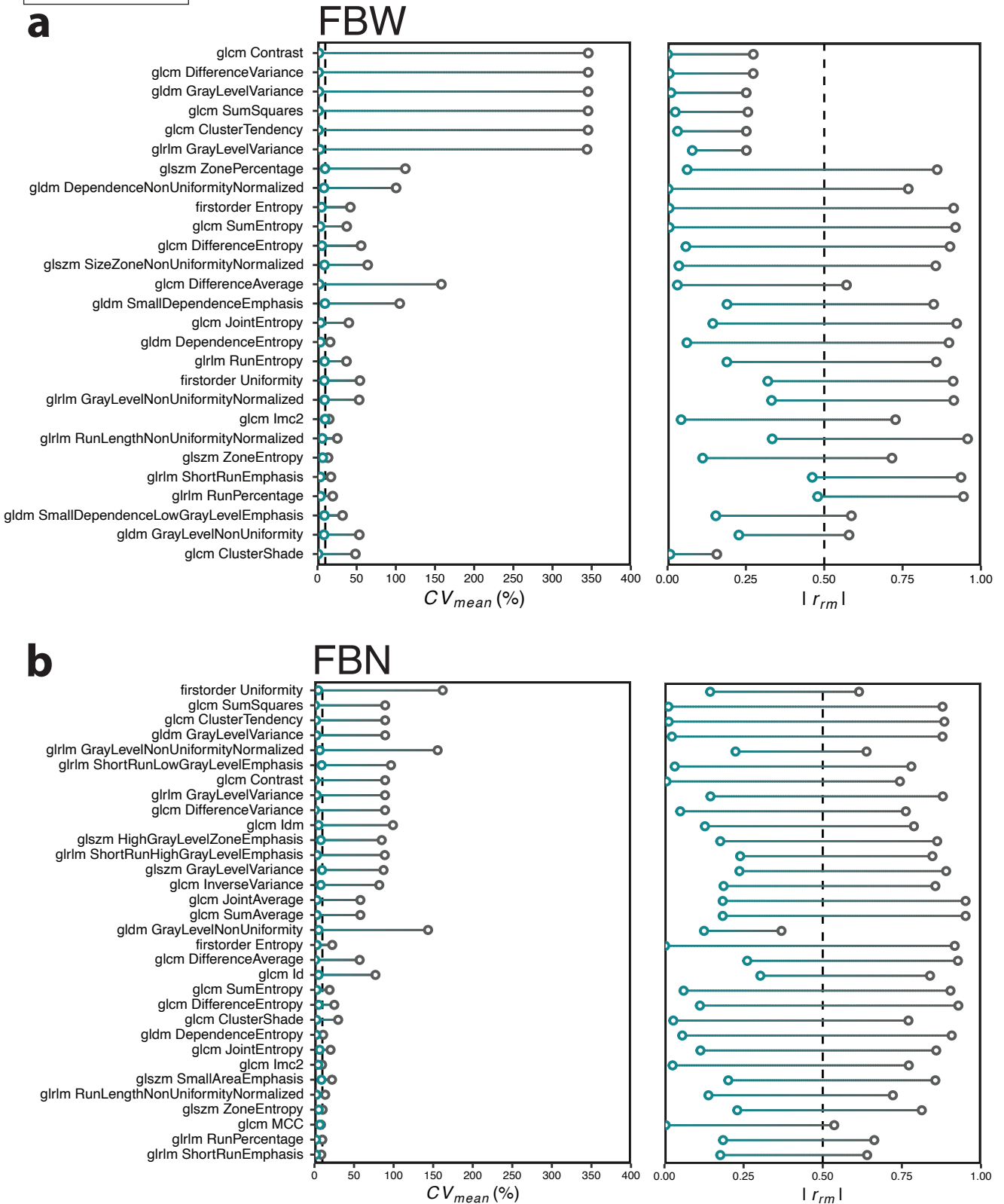
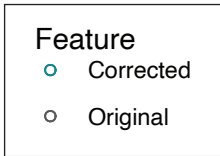


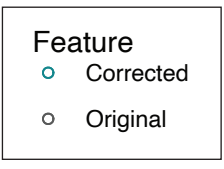
**f**



## Supplementary Figure SF9

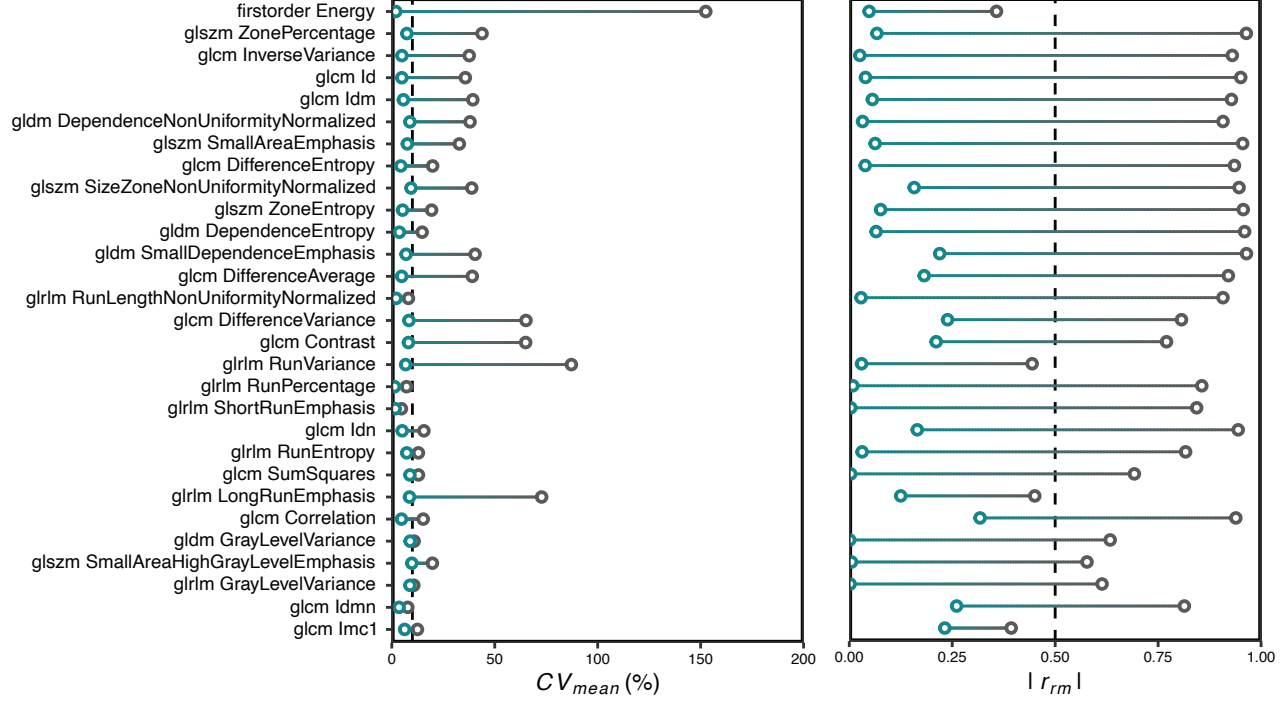
Dumbbell plots showing the change in  $CV_{mean}$  and  $|r_{rm}|$  for correctable features in lymphoma, when considering the different discretisation (a-b) and interpolation (c-f) algorithms tested. Features are ranked by the change in feature variability and correlation upon correction.





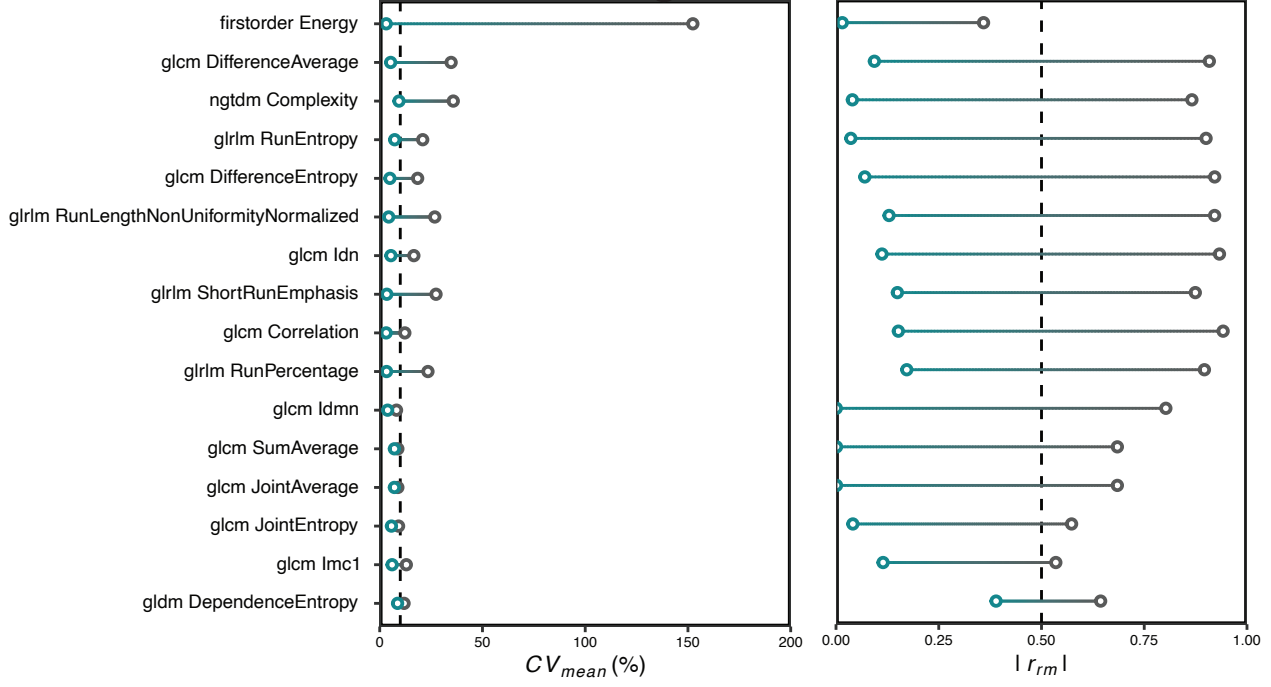
**c**

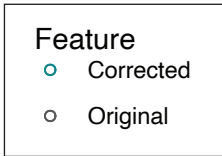
**Linear**



**d**

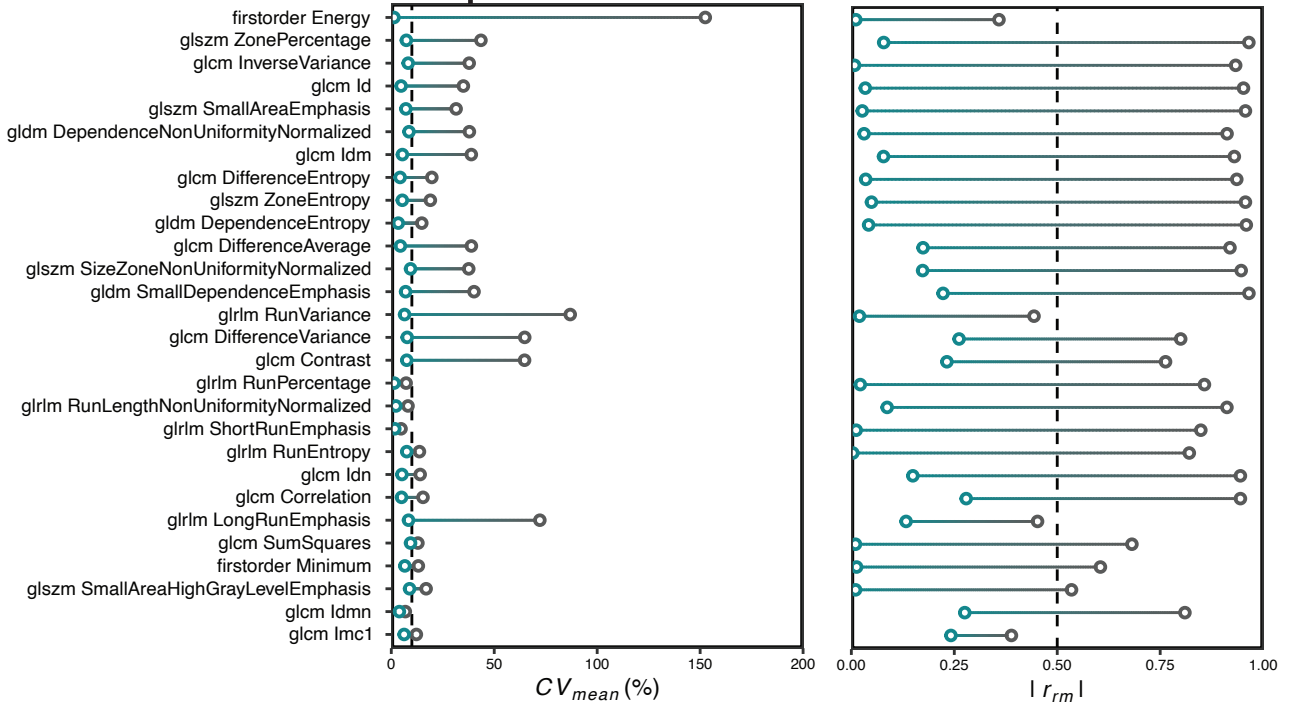
**Nearest-neighbour**





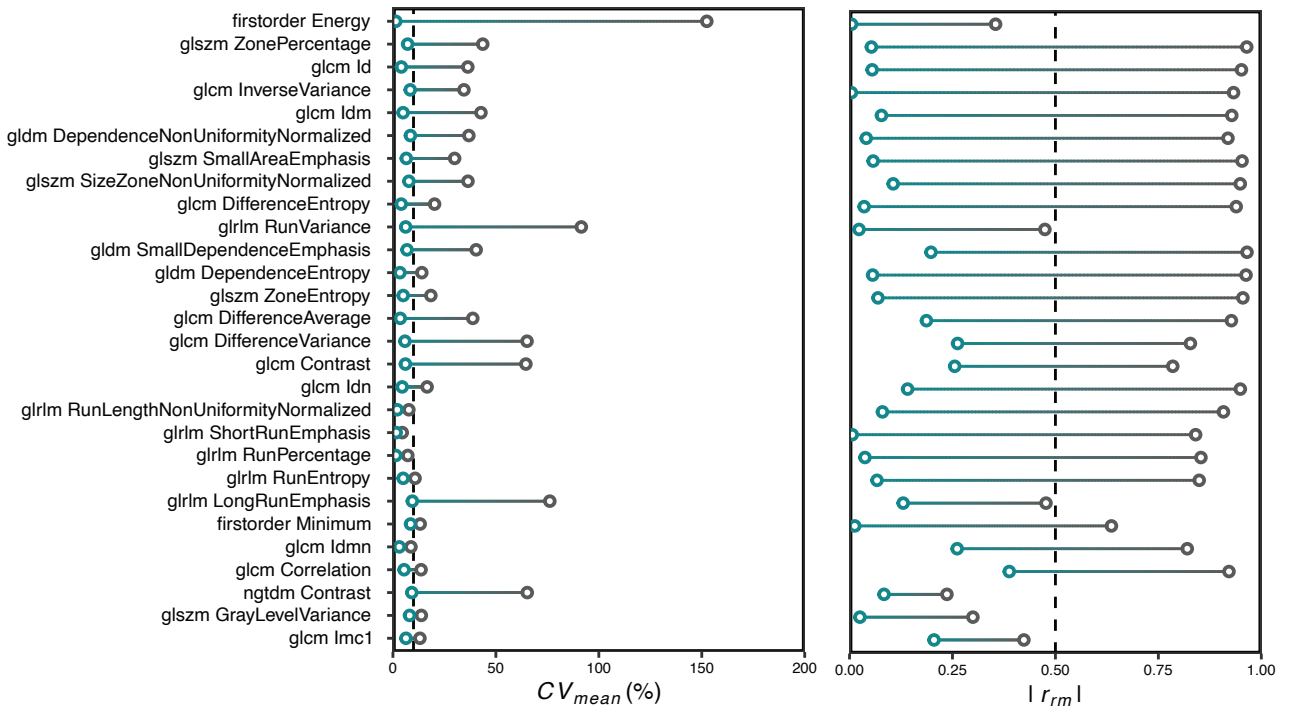
**e**

**B-spline**



**f**

**Gaussian**





## Supplementary Figure SF10

Density plots quantifying the overall effect of correction on feature variability and correlation for correctable features, stratified by image processing scheme and cancer type.

